Addition of Aryl and Fluoroalkyl Radicals to Fullerene C_{70}: ESR Detection of Five Regioisomeric Adducts and Density Functional Calculations†

Roberta Borghi,[1,‡] Lodovico Lunazzi,*[,‡] Giuseppe Placucci,[‡] Paul J. Krusic,*[,§] David A. Dixon,[§,⊥] Nobuyuki Matsuzawa,[∥] and Masafumi Ata[∥]

Contribution from the Department of Organic Chemistry "A. Mangini", University of Bologna, Risorgimento 4, Bologna 40136, Italy, Central Research and Development, E. I. du Pont de Nemours & Company, Wilmington, Delaware 19880-0328, and Sony Research Center, 174 Fujitsuka-cho, Hodogaya-ku, Yokahoma 240, Japan

Received March 25, 1996[⊗]

Abstract: The addition of several photochemically generated aryl and fluoroalkyl radicals to fullerene C_{70} was studied by electron spin resonance and the results were compared with those obtained with C_{60}. While simple alkyl radicals afford only three of the five expected $RC_{70}^{\bullet}$ regioisomers, the more reactive aryl and fluoroalkyl radicals give rise to four, except for the trifluoromethyl radical which yielded for the first time the ESR spectra of all five expected isomers. Semiempirical MO calculations and density functional theory calculations were carried out for $HC_{60}^{\bullet}$ and for the five $HC_{70}^{\bullet}$ regioisomers as models for the corresponding alkyl, aryl, and fluoroalkyl analogs in order to describe the unpaired electron distribution in these radical species and as an aid in the assignment of the observed spectra to specific $RC_{70}^{\bullet}$ regioisomers.

Introduction

In a preliminary communication[2] we reported an ESR study of the radical species obtained by single addition of a select number of simple free radicals, including the hydrogen atom, to fullerene C_{70}, and we compared the results with those for the analogous monoradical adducts derived from C_{60}. Unlike C_{60} where by virtue of its spherical symmetry only one monoadduct is obtained,[3] radical addition to ellipsoidal C_{70} can give rise to five isomeric $RC_{70}^{\bullet}$ adducts **A**, **B**, **C**, **D**, and **E**, named after the five distinct carbon atoms of C_{70} to which a radical can add (abundances 10:10:20:20:10). Initial work with alkyl radicals (*e.g. tert*-butyl)[4] and with muons[5,6] revealed the formation of only three of the possible five isomeric radical adducts. Later, four hydrogen atom[7] and muonium (Mu)[8] adducts were identified by ESR and muon spin rotation (μSR), respectively. More recently, all five possible C_{70}Mu isomers were observed by transverse field μSR.[9] In our work we also observed the formation of only three isomeric C_{70} monoadducts with simple alkyl radicals (*e.g.* methyl). The more reactive and electrophilic phenyl, trifluoromethyl, and pentafluoroethyl radicals, however, yielded four monoadducts in comparable relative abundances. Hoping to learn more about the elusive fifth isomeric adduct we examined in greater detail the addition of other aryl radicals to C_{70} and C_{60}.

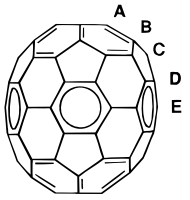

In addition to the identification of all possible regioisomers of $RC_{70}^{\bullet}$ radicals, there remain three particularly challenging interrelated questions: (a) the assignment of each individual spectrum dissected from the composite spectrum of all adducts to a specific regioisomer **A**, **B**, **C**, **D**, and **E**, (b) the description of the unpaired spin distribution in the various isomeric adducts, and (c) the measure of their relative stabilities. We approach the first question by an examination of the *g* factors and of spectral effects related to the symmetries of the various adducts and the remaining two by semiempirical and density functional molecular orbital calculations.

Computational Details

Because of the size of the systems, we used semiempirical molecular orbital theory to optimize the geometries. The calculations were done with the MNDO Hamiltonian[10] with the PM-3[11] parametrization as

† DuPont Contribution No. 7458.
‡ University of Bologna.
§ E. I. du Pont de Nemours & Company.
⊥ Present address: Pacific Northwest National Laboratory, Richland, Washington 99352.
∥ Sony Research Center.
⊗ Abstract published in *Advance ACS Abstracts,* August 1, 1996.

(1) In partial fulfillment of the requirements for the Ph.D. thesis in Chemical Sciences, University of Bologna.
(2) Borghi, R.; Lunazzi, L.; Placucci, G.; Krusic, P. J.; Dixon, D. A.; Knight, L. B., Jr. *J. Phys. Chem.* **1994**, *98*, 5395.
(3) (a) Morton, J. R.; Preston, K. F.; Krusic, P. J.; Hill, S. A.; Wasserman, E. *J. Phys. Chem.* **1992**, *96*, 3576. (b) Krusic, P. J.; Roe, D. C.; Johnson, E.; Morton, J. R.; Preston, K. F. *J. Phys. Chem.* **1993**, *97*, 1736.
(4) Keizer, P. N.; Morton, J. R.; Preston, K. F. *J. Chem. Soc., Chem. Commun.* **1992**, 1259.
(5) The positive muon is a short-lived particle ($\tau = 2.2$ μs) with a mass that is 1/9 that of a proton and a magnetic moment 3.1834 times that of the proton. Muonium is a muon bound to an electron that behaves as a light isotope of hydrogen.
(6) Niedermayer, C.; Reid, I. D.; Roduner, E.; Ansaldo, E. J.; Bernhard, C.; Binninger, U.; Glükler, H.; Recknagel, E.; Budnick, J. I.; Weidinger, A. *Phys. Rev. B* **1993**, *47*, 10923.
(7) Morton, J. R.; Negri, F.; Preston, K. F. *Chem. Phys. Lett.* **1994**, *218*, 467. See also: Klemt, R.; Roduner; Fischer, H. *Acta Chem. Scand.* Accepted for publication.
(8) Addison-Jones, B.; Percival, P. W.; Brodovitch, J.-C.; Ji, F.; Wlodek, S.; Selegue, J. P.; Meier, M. S.; Wakefield, J. B. *Hyperfine Interact.* **1994**, *86*, 817.
(9) Lappas, A.; Vavekis, K.; Prassides, K. *J. Chem. Soc., Chem. Commun.* **1994**, 2743.
(10) Stewart, J. J. P. *J. Comput. Aided Mol. Design* **1990**, *4*, 1.

S0002-7863(96)00979-1 CCC: $12.00

implemented in the program system MOPAC.[12] The semiempirical molecular orbital calculations were done with a spin restricted formalism because of problems in obtaining convergence of the spin unrestricted wave functions. Final energy and spin density calculations were done with the density functional theory program DGauss[13] on a Cray-C90 computer. The polarized double-ζ basis set[14] for C is of the form (721/51/1) (DZVP2) with a [7/3/3] fitting set and for H of the form (41/1) with a fitting basis set of the form (4). The calculations were done with an unrestricted spin formalism at the non-local (gradient-corrected) level with the non-local exchange potential of Becke[15] together with the non-local correlation functional of Perdew[16] (BP/DZVP2).

Experimental Section

The aryl and fluoroalkyl bromo derivatives employed in the present investigation were commercially available. The 3,5-dideuteriobromobenzene was prepared by reaction of 2 equiv of *n*-butyllithium with 1,3,5-tribromobenzene subsequently quenched with D_2O. Saturated solutions (~0.002 M) of pure C_{60} or C_{70} (>99% purity, obtained from Dynamic Enterprises, Ltd., Hanwell, Banbury, UK) in benzene or *tert*-butylbenzene containing from 1 to 20 equiv of aryl halides (Br, I) were prepared free of oxygen either by the use of previously carefully dried and degassed solvents in a nitrogen-flushed glovebox (Vacuum Atmospheres Co.) or by careful degassing in a high-vacuum system. The gaseous fluoroalkyl bromides were handled in a vacuum system and were metered in a flask of known volume. The pressure was read by an MKS Instruments Inc. Baratron capacitance manometer. The desired number of moles calculated from the ideal gas law were condensed in a sample tube equipped with a Teflon high-vacuum stopcock. The samples contained in 4- or 5-mm o.d. quartz tubes were irradiated in the standard X-band microwave cavity of the ESR spectrometer, equipped with a quartz insert for variable-temperature work, with the focussed light of a 500-W high-pressure mercury lamp (Bologna) or of a 500-W Cermax Xenon Illuminator (DuPont). The light was filtered through a 5-cm path of either circulating distilled water (strongest signals) or circulating aqueous Kasha filter (240 g/L of $NiSO_4 \cdot 6H_2O$, 45 g/L $CoSO_4 \cdot 7H_2O$) to reduce the heating of the sample.[17] The temperatures read by the variable-temperature apparatus were corrected for heating caused by irradiation. ESR spectra were obtained by using Varian E4 (Bologna) or Bruker ESP-300 spectrometers. Because of the extremely narrow widths of the spectral lines, very low microwave powers (<200 μW) and magnetic field modulations (<80 mG) were used. The relative *g* factors of the various isomeric C_{70} radical adducts and their relative populations were established by careful computer simulation of each composite spectrum. The *g* factors of the C_{60} adducts were measured by comparison with the line due to the C_{60} excited triplet, whose *g* factor is 2.00135,[18] which can be detected simultaneously when substoichiometric amounts of aryl bromides were used. The *g* factors of the C_{70} adducts were measured relative to the spectrum of the corresponding $Ar-C_{60}^{\bullet}$ radical derived from C_{60} either present as low-level impurity in C_{70} or added in controlled amounts to the C_{70} solutions. At DuPont the *g* factors were determined by precise measurement of the magnetic field with a Bruker tracking gaussmeter and of the microwave frequency with a 5350B Hewlett-Packard frequency counter. The difference in magnetic field between the gaussmeter probe location and the center of the cavity was established by means of a perylene$^{\bullet+}$/concentrated H_2SO_4 standard in a capillary tube ($g = 2.002569$).[19] The errors are believed not to exceed ±0.00003.

Table 1. ESR Parameters of the Radical Adducts $Ar-C_{60}^{\bullet}$ [a]

radical	Ar	a_H (G)	a_F (G)	*g* factor
1	phenyl	0.22 (2H)		2.00222
1′	3.5-dideuteriophenyl			2.00222
2	3-methylphenyl	0.23 (1H)		2.00222
3	3,5-dimethylphenyl			2.00221
4	4-methylphenyl	0.22 (2H)		2.00222
5	3,5-difluorophenyl		0.60 (2F)	2.00229
6	3-fluorophenyl	0.29 (1H)	0.50 (1F)	2.00223
7	4-fluorophenyl	0.20 (2H)		2.00230
8	1-naphthyl	0.25 (2H)[b]		2.00229
9	2-naphthyl	0.18 (1H)		2.00220
10	9-phenanthryl	0.26 (1H)		2.00226

[a] In benzene solution at 298 K. [b] At very high resolution two smaller splittings of 0.07 and 0.03 G, each due to a single proton, are also detected.

Results

Electron Spin Resonance. Intense UV photolysis of dilute benzene solutions containing C_{60} and C_6H_5-X (X = Br, I, or HgC_6H_5) produces the radical adduct $C_6H_5-C_{60}^{\bullet}$ (**1**, Table 1) whose ESR spectrum is a 1:2:1 triplet (0.22 G) due to the hyperfine interaction of the unpaired electron with the pair of phenyl protons in the meta position. This assignment is established by the spectral changes that are observed when these protons are replaced by various substituents. Thus, addition of the aryl radicals obtained from 3-methylbromobenzene and 3,5-dimethylbromobenzene to C_{60} yields the adducts **2** and **3** whose spectra display a doublet and a singlet since only one hydrogen or none are left in the meta position, respectively. A binomial triplet is observed again for radical **4** obtained by photolysis of C_{60} and 4-methylbromobenzene as both meta protons are present. As expected, substitution of both meta protons with two deuterons in **1′**, obtained by photolysis of C_{60} and 3,5-dideuteriobromobenzene, yields a single-line ESR spectrum.

A relatively strong hyperfine interaction in the meta position and no measurable interaction in the ortho and para positions is revealed also by fluorophenyl analogs. Thus, 3,5-difluorobromobenzene reacts with C_{60} to give adduct **5** displaying only a hyperfine interaction of 0.60 G for two equivalent fluorines, while 3-fluorobromobenzene yields radical **6** with a doublet-of-doublets for one meta fluorine (0.50 G) and one meta proton (0.29 G). A slightly larger F hyperfine interaction compared with a proton interaction in the same position in aromatic radicals is well established. Finally, no fluorine hyperfine splitting is detected for radical **7**, derived from 4-fluorobromobenzene, since the fluorine now occupies the para position, and only the splitting due to two equivalent meta protons is observed.

The products of photoreaction of C_{60} with 1- and 2-bromonaphthalene agree with the above behavior of hyperfine splittings. In radical **8** the 1-naphthyl substituent bears two meta-like protons in positions 3 and 8 and thus displays a triplet spectrum (0.25 G, Figure 1). At much higher resolution the equivalence is not complete, as evidenced by a broadened central line of the 1:2:1 triplet, and two additional smaller splittings (0.07 G and 0.03 G), each due to single protons, can be discerned. In radical **9**, on the other hand, the 2-naphthyl

(11) (a) Stewart, J. J. P. *J. Comput. Chem.* **1989**, *10*, 209. (b) Stewart, J. J. P. *J. Comput. Chem.* **1989**, *10*, 221.
(12) Stewart, J. J. P. QCPE Program 455, 1983; Version 5.0.1.
(13) (a) Andzelm, J.; Wimmer, E.; Salahub, D. R. *The Challenge of d and f Electrons: Theory and Computation*, Salahub, D. R., Zerner, M. C., Eds.; ACS Symposium Series, No. 394; American Chemical Society: Washington, DC, 1989; p 228. (b) Andzelm, J. In *Density Functional Theory in Chemistry*; Labanowski, J., Andzelm, J., Eds.; Springer Verlag: New York, 1991; p 155. (c) Andzelm, J.; Wimmer, E. *J. Chem. Phys.* **1992**, *96*, 1280. (d) DGauss is a density program available via the Cray Inichem Project.
(14) Godbout, N.; Salahub, D. R.; Andzelm, J.; Wimmer, E. *Can. J. Chem.* **1992**, *70*, 560.
(15) (a) Becke, A. D. *Phys. Rev. A* **1988**, *38*, 3098. (b) Becke, A. D. In *The Challenge of d and f Electrons: Theory and Computation*; Salahub, D. R., Zerner, M. C., Eds.; ACS Symposium Series, No. 394; American Chemical Society: Washington, DC, 1989; p 166. (c) Becke, A. D. *Int. J. Quantum Chem. Symp.* **1989**, *23*, 599.
(16) Perdew, J. P. *Phys. Rev. B* **1986**, *33*, 8822.
(17) Kasha, M. *J. Opt. Soc. Am.* **1948**, *38*, 929.
(18) Closs, G. L.; Gautman, P.; Zhang, D.; Krusic, P. J.; Hill, S. A.; Wasserman, E. *J. Phys. Chem.* **1992**, *96*, 5228.
(19) Segal, B. G.; Kaplan, M.; Fraenkel, G. K. *J. Chem. Phys.* **1965**, *43*, 4191.

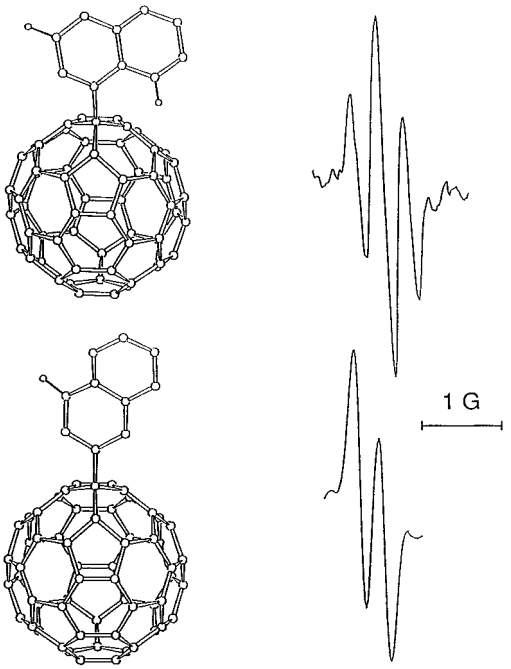

Figure 1. ESR spectra of 1-naphthyl−$C_{60}^{\bullet}$ (**8**) (top) and 2-naphthyl−$C_{60}^{\bullet}$ (**9**) radicals in benzene at 295 K. Only the meta-like hydrogens, responsible for the triplet and doublet splittings, respectively, are shown in the structures.

substituent has only a single meta proton in position 4 that accounts for the observed doublet spectrum (Figure 1). Similarly, the photoreaction of C_{60} with 9-bromophenanthrene yields radical **10** which displays a doublet spectrum since the proton in position 1 of the 9-phenanthryl moiety is the only one which occupies a meta-like position.

The reasons for the relatively large meta splittings accompanied by negligible splittings in the ortho and para positions are unclear. It should be recalled, however, that σ radicals, such as the benzoyl radical $C_6H_5-CO^{\bullet}$, similarly display ortho and para proton splittings much smaller than those of meta protons[20,21] and that unusual long-range interactions were observed for the adamantyl and bicyclooctyl C_{60} radical adducts[3a] suggesting that effects similar to those described by the W plan[22] in long-range hyperfine interactions are operative.

Similar photoreactions of aryl bromides, iodides, and aryl mercury compounds with C_{70} yielded composite spectra from which the individual spectra of four isomeric species could be dissected. The correctness of this analysis was verified by careful computer simulations which yielded the precise spectral parameters of four regioisomers, including their relative *g* factors and their relative abundances. The latter do vary somewhat with the temperature and sample composition and cannot be taken as reliable indicators of the relative thermodynamic stabilities of the isomers. The analysis was made possible by the unusual narrowness of the spectral lines together with the small but significant changes in the *g* factors for the different isomers which noticeably shift the component spectra one with respect to the other. The splitting patterns are the same as those of the C_{60} analogs differing only slightly in the magnitudes of the splittings.

The spectrum obtained in the photoreaction of C_{70} with diphenylmercury in benzene[23] is shown in Figure 2A together with the computer simulation based on the parameters in Table 2 for four isomers **I**, **II**, **III**, and **IV**, labeled in the order of decreasing relative abundances. Each isomer gives rise to a triplet for two meta protons with a splitting that is very similar

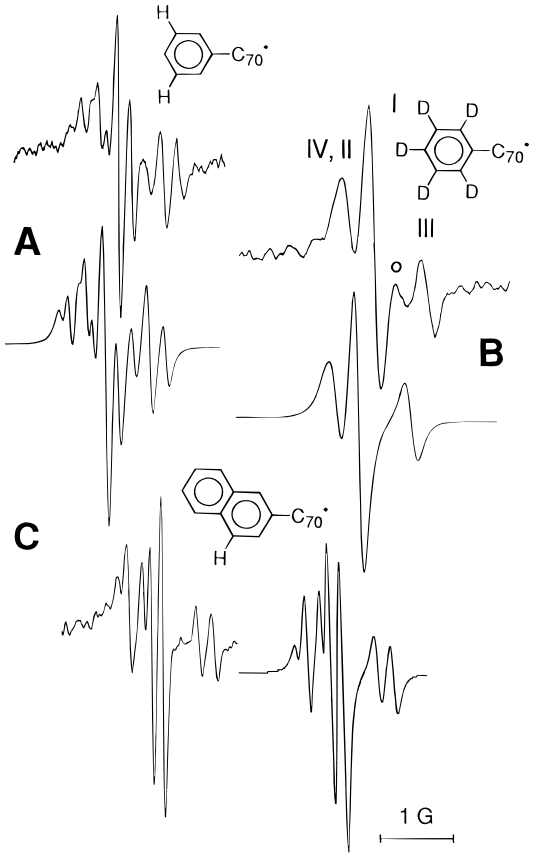

Figure 2. Composite ESR spectra (benzene, 295 K) and their computer simulations of four isomers of $C_6H_5C_{70}^{\bullet}$(**11**) (**A**), $C_6D_5C_{70}^{\bullet}$ (**B**), and 2-naphthyl−$C_{70}^{\bullet}$(**15**) (**C**).

Table 2. ESR Parameters of the Radical Adducts Ar−$C_{70}^{\bullet}$ [a]

radical	Ar	rel %	a_H (G)	a_F (G)	*g* factor
11	phenyl	**I** (45)	0.18 (2H)		2.00248
		II (25)	0.24 (2H)		2.00266
		III (20)	0.24 (2H)		2.00207
		IV (10)	0.27 (2H)		2.00272
12	3,5-difluoro-phenyl	**I** (45)		0.60 (2F)	2.00251
		II (31)		0.64 (2F)	2.00268
		III (10)		0.78 (2F)	2.00215
		IV (14)		0.71 (2F)	2.00277
13	3-fluorophenyl	**I** (46)	0.24 (1H)	0.46 (1F)	2.00242
		II (33)	0.26 (1H)	0.52 (1F)	2.00261
		III (13)	0.30 (1H)	0.56 (1F)	2.00202
		IV (8)	0.16 (1H)	0.33 (1F)	2.00283
14	1-naphthyl	**I** (15)	0.27 (2H)		2.00240
		II (25)	0.27 (2H)		2.00262
		III (35)	0.28 (2H)		2.00201
		IV (25)	0.31 (2H)		2.00266
15	2-naphthyl	**I** (57)	0.17 (1H)		2.00243
		II (27)	0.20 (1H)		2.00262
		III (10)	0.22 (1H)		2.00201
		IV (6)	0.25 (1H)		2.00269
16	9-phenanthryl	**I** (67)	0.27 (1H)		2.00244
			0.16 (1H)		
		II (7)	0.34 (1H)		2.00262
		III (19)	0.29 (1H)		2.00206
			0.08 (1H)		
		IV (7)	0.30 (1H)		2.00269

[a] In benzene solution at 298 K.

(20) Krusic, P. J.; Rettig, T. A. *J. Am. Chem. Soc.* **1970**, *92*, 722.
(21) Grossi, L.; Placucci, G. *J. Chem. Soc., Chem. Commun.* **1985**, 943.
(22) Russell, G. A.; Chang, K. Y. *J. Am. Chem. Soc.* **1965**, *87*, 4381. Russell, G. A.; Chang, K. Y.; Jefford, C. W. *J. Am. Chem. Soc.* **1965**, *87*, 4383. Norman, R. O. C.; Gilbert, B. C. *J. Phys. Chem.* **1967**, *71*, 14. King, F. W. *Chem. Rev.* **1976**, *76*, 157.

(23) An analogous spectrum was obtained using iodobenzene.

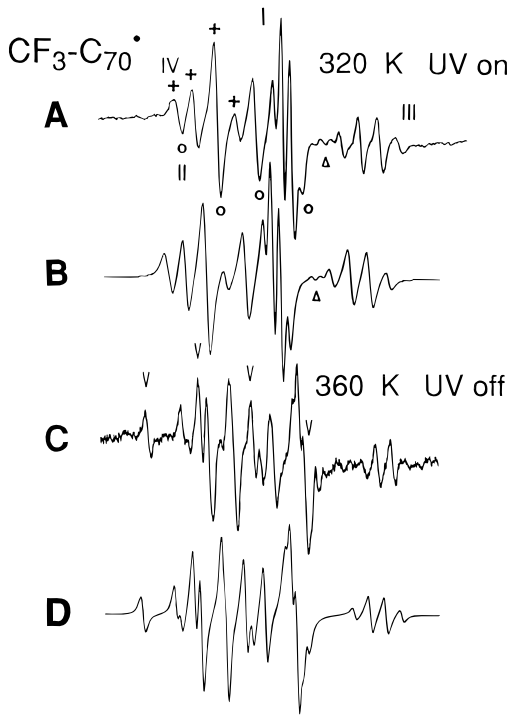

Figure 3. (A) ESR spectrum and its computer simulation (B, using the parameters in Table 3) obtained during UV irradiation of C_{70} and CF_3Br in benzene showing four quartets labeled with Roman numerals belonging to four regioisomers of $CF_3C_{70}^{\bullet}$. The lines of quartet **II** are marked with circles and those of quartet **IV** with crosses. The triangle in A denotes a weak quartet belonging to $CF_3C_{60}^{\bullet}$ which has also been accounted for in the simulation (B). (C) ESR spectrum and its simulation (D) obtained by raising the temperature to 360 K in the dark after UV irradiation at room temperature showing a fifth quartet labeled with the symbols V belonging to the fifth isomer of $CF_3C_{70}^{\bullet}$.

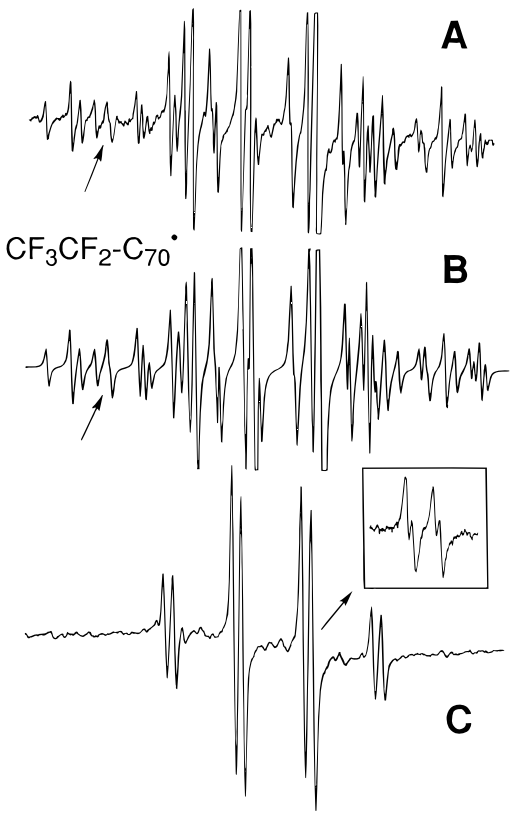

Figure 4. ESR spectrum obtained by UV irradiation of C_{70} and CF_3-CF_2Br in 1,2,3-trichlorobenzene at 380 K (A). The spectrum was simulated (B) with the parameters of Table 3 as a superposition of the spectra of four distinct regioisomers of $CF_3CF_2C_{70}^{\bullet}$. The arrows point to a crucial inflection revealing the lack of symmetry in one regioisomer (see text). The spectrum of one regioisomer (part **C**) persists on shuttering the light (340 K). This isomer also lacks symmetry since the spectrum reveals two differet CF_2 fluorines (doublet-of-doublets, see inset).

to that observed for the C_{60} analog, but only **11(III)** has a *g* factor that approaches that of $C_6H_5-C_{60}^{\bullet}$ (2.00207 *vs* 2.00222) while the fourth and least abundant isomer **11(IV)** has a *g* factor which is by ESR standards quite different (2.00272) (Table 1). Figure 2B shows the composite spectrum of the deuterated analogs wherein each triplet has collapsed to a broader single line since the meta deuterons' hyperfine interaction, a quintet for two equivalent $I = 1$ nuclei, is reduced by a factor of 6.5144 (the proton−deuteron magnetic moment ratio) relative to the corresponding proton interaction. The observation of detectable amounts of $C_6D_5-C_{60}^{\bullet}$ (line marked with a circle in Figure 2B), in spite of the high purity of the starting C_{70}, gives qualitative evidence of the much higher reactivity of C_{60} toward free radicals.

Analogous composite spectra were obtained when C_{70} was reacted with several other photochemically generated aryl radicals and were similarly analyzed by computer simulation as illustrated in Figure 2C for the 2-naphthyl−C_{70} isomeric radical adducts. In each case the spectra were due to four isomeric adducts whose ESR parameters are gathered in Table 2. The labeling of the isomers using Roman numerals maintains the same ordering of *g* factors observed for the regioisomers of $C_6H_5-C_{70}^{\bullet}$ although this ordering does not always correspond to decreasing relative abundances. The behavior of the *g* factors ordered in this fashion is striking: an average increase of 0.000 19(±2) (standard deviation in the last digit) from **I** to **II** is followed by an average decrease of 0.000 58(±3) from **II** to **III**, which in turn is followed by another average increase of 0.000 67(±6) from **III** to **IV**. We conclude that the isomers with the same Roman numeral are structurally analogous to each other.

Trifluoromethyl and pentafluoroethyl radicals from the photolysis of the corresponding bromo derivatives[24] also add readily to C_{70} as they do to C_{60}.[25] Simulation of the composite spectra (Figures 3 and 4) shows the presence of four regioisomers in comparable abundances during UV irradiation. The spectra of the $CF_3-C_{70}^{\bullet}$ isomers are all quartets (Table 3) for three equivalent fluorines above 285 K indicating that at these temperatures the CF_3 group in all four regioisomers is rotating freely about the bond connecting it to the C_{70} surface. Isomers **I**, **II**, **III**, and **IV** have exactly the same relative disposition of the *g* factors as the aryl adducts **I** through **IV** and are therefore their structural analogs. The fluorine splittings of the $CF_3-C_{70}^{\bullet}$ isomers (absolute values of the hyperfine interactions) are slightly temperature dependent: the temperature coefficients (∼0.5 mG/K) are negative for **I**, positive for **II**, negative for **III**, and positive for **IV** and compare with a positive temperature coefficient of $|a(F)|$ for $CF_3-C_{60}^{\bullet}$ (∼0.75 mG/K).[25c] Upon shuttering the light at 320 K the spectra of **II**, **III**, and **IV** are not detected while the spectrum of **I** grows in intensity, and a new weaker quartet spectrum appears with the relatively high *g* factor of 2.00280 and a CF_3 fluorine splitting of 0.33 G with a positive temperature coefficient. If the temperature is now raised with no further irradiation to 360 K the spectra of isomers

(24) Perfluoroethyl radicals were also generated by photolysis or thermolysis of perfluoropropionyl peroxide C_2F_5-C(O)O-O(O)C-C_2F_5.

(25) (a) Fagan, P. J.; Krusic, P. J.; Mc Ewen, C. N.; Lazar, J.; Parker, D. H.; Herron, N.; Wasserman, E. *Science* **1993**, *262*, 404. (b) Morton, J. R.; Preston, K. F. *J. Phys. Chem.* **1994**, *98*, 4993. (c) Krusic, P. J.; Kleier, D, To be submitted for publication.

Table 3. ESR Parameters of the Radical Adducts R_F-$C_{60}^{\bullet}$ and R_F-$C_{70}^{\bullet}$ [a,b]

radical	rel %	a_F (G, abs values)	*g* factor	*T* (K)
$CF_3C_{60}^{\bullet}$		0.070(3F)	2.00235	320
		0.145 (3F)		380
$CF_3C_{70}^{\bullet}$	**I** (37)	0.05 (3F)	2.00251	320
	II (26)	0.25 (3F)	2.00271	320
	III (16)	0.13 (3F)	2.00218	320
	IV (21)	0.13 (3F)	2.00283	320
	I (35)	0.035 (3F)	2.00251	360
	II (16)	0.273 (3F)	2.00271	360
	III (7)	0.100 (3F)	2.00218	360
	IV (22)	0.165 (3F)	2.00283	360
	V (20)	0.330 (3F)	2.00280	360
$CF_3CF_2C_{60}^{\bullet}$		0.35 (2F); 2.45 (3F)		260[c]
		0.53 (2F); 2.25 (3F)	2.00235	450[d]
$CF_3CF_2C_{70}^{\bullet}$ [d]	**I** (31)	0.20 (1F);0.04 (1F)	2.00240	380
		1.35 (3F)		
	II (26)	0.58 (1F); 0.63 (1F)	2.00260	380
		2.13 (3F)		
	III (20)	0.125 (2F); 2.27 (3F)	2.00202	380
	IV (23)	0.53 (2F); 2.52 (3F)	2.00273	380

[a] Generated in benzene solutions by photolysis of the corresponding fluoroalkyl bromide unless noted otherwise. [b] Line widths ~ 30 mG. [c] In *tert*-butylbenzene. [d] In 1,2,4-trichlorobenzene.

II, **III**, and **IV** grow in affording a composite spectrum of *five* CF_3 fluorine quartets (Figures 3C and 3D). We assign the new quartet (marked with V symbols in Figure 3C) with the high *g* factor of 2.00280 and fluorine hyperfine splitting of 0.33 G (Table 3) to the elusive fifth isomer which is evidently unstable under UV irradiation under our experimental conditions possibly due to reversible addition of the CF_3 radical. The photochemistry in these systems is quite complex. With excess CF_3I and C_{60} in benzene, for example, we detected by mass spectrometry substantial hydrogenation of the $(CF_3)_nC_{60}$ products and the formation of appreciable amounts of α-trifluorotoluene.[25a] The above behavior indicates that isomers **II**, **III**, and **IV** dimerize readily on shuttering the light to diamagnetic dimers invisible by ESR that can dissociate back into paramagnetic monomers by raising the temperature in a fashion analogous to their C_{60} analogs.[26] The persistency of **I** and **V** at relatively low temperatures and in the absence of UV irradiation also indicates that isomers of this type are intrinsically less prone to dimerization than those of type **II**, **III**, and **IV**.

The more complicated composite spectrum of the $CF_3CF_2-C_{70}^{\bullet}$ isomeric adducts is again the superposition of the spectra of four isomers as can be verified by computer simulation (Figures 4A and 4B). Their *g* factors fall exactly into the familiar pattern found above for the previous adducts so that they can also be numbered with Roman numerals denoting isostructural isomers (Table 3). The spectra of isomers **III** and **IV** have the same splitting pattern as the C_{60} analog: a quartet-of-triplets for three equivalent CF_3 fluorines and two equivalent CF_2 fluorines up to 470 K (high-temperature experiments in 1,2,3-trichlorobenzene solvent). Isomers **I** and **II**, however, are different: in **I** only one of the two CF_2 fluorines interacts appreciably (0.20 G at 340 K) while the second has a splitting that can barely be resolved (0.040 G at 273 K with the light off, inset in Figure 4C) while in **II** the two CF_2 fluorines are equivalent at 450 K *but not* at 380 K (0.58 and 0.63 G).[27] Though the inequivalence is very slight, it nevertheless causes an unmistakable break in the line indicated by an arrow in Figure 4A. The observation of two distinct CF_2 fluorines in $CF_3CF_2-C_{70}^{\bullet}$(**I**) and $CF_3CF_2-C_{70}^{\bullet}$(**II**) demands that these two radicals, and consequently all homologous isomers **I** and **II**, *be without a plane of symmetry* and that the fluoroethyl group be not free to rotate around the bond connecting it to the C_{70} surface even at temperatues as high as 470 K. The latter agrees with the behavior of fluoroalkyl radical adducts of C_{60} higher than the trifluoromethyl adduct, such as perfluoroethyl, perfluoroisopropyl, perfluoro-*n*-butyl, and perfluoro-*tert*-butyl, in which the fluoroalkyl substituent is essentially locked in a preferred staggered conformation relative to the C_{60} framework below it on the time scale of the ESR experiment ($<\sim 1$ μs) as appropriate for barriers of the order of 10 kcal/mol.[25c,28] Because of these high barriers to internal rotation in $R_F-C_{60}^{\bullet}$ radicals, the observation of two equivalent CF_2 fluorines in **III** and **IV** cannot be due to free rotation but rather to the presence of a plane of symmetry in the isomers of type **III** and **IV**. Unfortunately, we were not able to detect the fifth isomer of $CF_3CF_2-C_{70}^{\bullet}$ by shuttering the light. Instead, a quality spectrum of $CF_3CF_2-C_{70}^{\bullet}$(**I**) unencumbered by the spectra of other isomers was recorded at 340 K (Figure 4C) underscoring the reluctance of isomers of type **I** to dimerize.

The striking regularity in the disposition of *g* factors used to place the C_{70} radical adducts discussed so far into isostructural groups labeled by the same Roman numeral can be extended to other C_{70} radical monoadducts including the C_{70} monohydrides (Table 6) and the methyl[2] and the *tert*-butyl[4] adducts. Based on eleven sets of $R-C_{70}^{\bullet}$ isomers, radicals of type **I** have an average *g* factor of $2.00246 \pm 6 \times 10^{-5}$, those of type **II** of $2.00265 \pm 5 \times 10^{-5}$, those of type **III** of $2.00207 \pm 8 \times 10^{-5}$, and those of type **IV** of $2.00276 \pm 7 \times 10^{-5}$. The only existing C_{70} radical adduct of type **V** has the *g* factor 2.00280. The *g* factor is thus determined more by the regiochemistry of the radical adduct than by the nature of the alkyl or fluoroalkyl group that has attached itself to C_{70}. Probably this is because of the very small unpaired electron delocalization onto the R and R_F groups as judged by the very small proton and fluorine hyperfine splittings in these radicals.

Electronic Structure Calculations. (a) Semiempirical MO Calculations. Although it would be desirable to calculate geometric and electronic structures of molecules with as rigorous a theory as possible, *ab initio* molecular orbital (MO) or density functional theory (DFT) methods with reasonable basis sets would be computationally too expensive to use to fully optimize the geometry for open-shell systems such as the $HC_{70}^{\bullet}$ isomers with little or no symmetry as models for other $R-C_{70}^{\bullet}$ radical adducts. We therefore carried out geometry optimizations with a semiempirical method and then used these geometries for DFT calculations of the spin densities and energies. Calculations were carried out with the PM-3 parametrization of the MNDO Hamiltonian using the MOPAC program system for the five isomers **A**, **B**, **C**, **D**, and **E** of the $HC_{70}^{\bullet}$ radical. We have previously reported the results of similar calculations on $HC_{60}^{\bullet}$ and other C_{60} adducts.[29]

The optimized structures are shown in Figure 5 together with that of $HC_{60}^{\bullet}$ from our previous work.[29] A detailed examination of the bond lengths shows that the only significant structural changes relative to C_{70} and C_{60} upon H atom addition occur in the immediate vicinity of the carbon bearing the hydrogen. The carbon bonded to H extrudes somewhat from the ellipsoidal or

(26) Morton, J. R.; Preston, K. F.; Krusic, P. J.; Hill, S. A.; Wasserman, E. *J. Am. Chem. Soc.* **1992**, *114*, 5454.

(27) Elevated temperatures using 2,3,5-trichlorobenzene as solvent produced spectra of higher intensity in this case because the dimerization equilibrium is shifted in favor of the radical monomers.

(28) The claim in ref 25b that in $(CF_3)_2CF-C_{60}^{\bullet}$ there is rapid exchange between two asymmetric conformations even at 150 K is erroneous and counterintuitive and affects catastrophically the considerations concerning the signs of the fluorine hyperfine coupling constants and of their temperature coefficients based on this assumption.[25c]

(29) Matsuzawa, N.; Dixon, D. A.; Krusic, P. J. *J Phys. Chem.* **1992**, *96*, 8317.

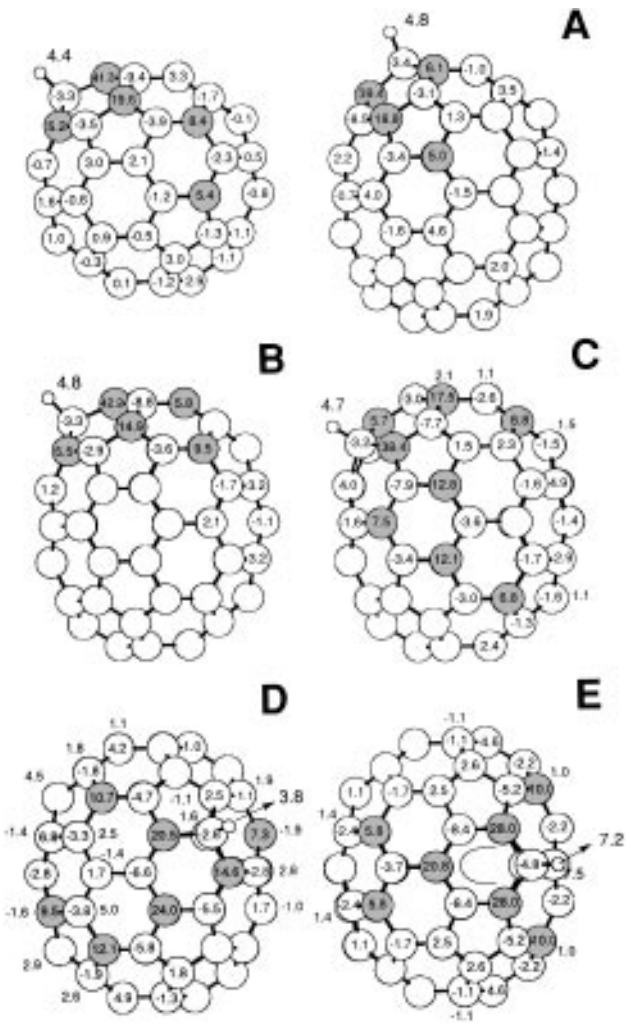

Figure 5. Unpaired spin densities (greater than 1% except for $HC_{60}^{\bullet}$) by density functional theory calculations in $HC_{60}^{\bullet}$ (top left) and in the five distinct $HC_{70}^{\bullet}$ regioisomers (**A** through **E**). The structures showing one hemisphere are MNDO/PM-3 energy optimized. For $HC_{60}^{\bullet}$ (top left), isomer **A**, and isomer **B** the page is the plane of symmetry, for **E** the plane of symmetry is perpendicular to the page, and for **C** and **D** there is no symmetry. The smaller numbers next to the circles representing carbon atoms are the unpaired spin densities for the carbons directly below on the opposite hemisphere. The shading identifies carbon atoms with more than 5% positive unpaired spin density.

spherical surfaces of C_{70} and C_{60}, respectively, as expected for an essentially sp^3-hybridized carbon connected to three contiguous carbons on the curved surfaces by typical single bonds (1.52 $\pm$ 0.02). This localized geometrical distortion has emerged from other semiempirical[7,8,30] and *ab initio calculations*[31] on $HC_{70}^{\bullet}$ and $HC_{60}^{\bullet}$ and their muonium analogs. Although the CC bond lengths are as expected, the CH bond lengths at the PM-3 level are longer than in alkanes (1.116 $\pm$ 0.001 Å except for **E** for which d(CH) = 1.123 Å). These values are in good agreement with the value of 1.113 Å calculated for the unique hydrogen (eclipsing the singly occupied orbital) in $CH_3CH_2^{\bullet}$ of C_{2v} symmetry at the nonlocal DFT level. Figure 5 also shows quite clearly the great structural similarity between $HC_{60}^{\bullet}$ and $HC_{70}^{\bullet}$ (**B**) and the dissimilarity between $HC_{60}^{\bullet}$ and $HC_{70}^{\bullet}$(**A**) at the polar cap, that is also reflected in the unpaired spin density

(30) (a) Percival, P. W.; Wlodek, S. *Chem. Phys. Lett.* **1992**, *196*, 317. (b) Reid, I. D.; Roduner, E. *Hyperfine Interact.* **1994**, *86*, 809. (c) Morton, J. R.; Negri, F.; Preston, K. F. *Can. J. Chem.* **1994**, *72*, 776.

(31) (a) Claxton, T. A.; Cox, S. F. J. *Chem. Phys. Lett.* **1993**, *207*, 31. (b) Claxton, T. A.; Graham, J. *J. Chem. Phys.* **1993**, *97*, 4621. (c) Estreicher, S. K.; Latham, C. D.; Heggie, M. I.; Jones, R.; Öberg *Chem. Phys. Lett.* **1992**, *196*, 311.

Table 4. MNDO/PM-3 and NLDFT Relative Energies of the $HC_{70}^{\bullet}$ Isomers in kcal/mol

isomer	$\Delta\Delta H$(PM-3)	ΔE(NLDFT)
A	1.6	0.0[b]
B	2.5	1.2
C	0.0[a]	1.9
D	0.4	0.4
E	15.6	7.8

[a] $\Delta H_f°$(calc) = 885.8 kcal/mol. [b] E_{elec} = −2668.710558 au.

distributions (*vide infra*), as well as the presence of a plane of symmetry for **A**, **B**, and **E** and no symmetry element for **C** and **D**.

The relative energies calculated at the MNDO/PM-3 level for the five isomeric forms of $HC_{70}^{\bullet}$ are presented in Table 4. Since small energy differences at this level of computation are not significant, one can only say that there are four isomers of approximately the same energy, all of which are substantially more stable than the equatorial adduct **E**. This order of stabilities was found previously[7,30b,32] and the same order was predicted for the analogous isomers of the anionic HC_{70}^{-} hydride.[33] The result that isomer **E** is the least stable isomer can be rationalized by consideration of the Kekulé structure of C_{70}[34] shown above. While there is a clear distinction between single and double bonds, that is long and short bonds, near the polar caps that most resemble C_{60}, the distinction is lost at the equatorial belt made up of fused six-membered rings. The five six-membered rings on the equator are essentially equilateral and therefore benzene-like. Consequently, radical addition to the equatorial carbons **E** leads to a cyclohexadienyl-like radical, a picture that is supported by the spin density calculations (*vide infra*), and therefore to the loss of local aromatic resonance stabilization.

(b) Density Functional Theory Calculations. Due to convergence problems at the UHF level for $C_{60}H^{\bullet}$ and $C_{70}H^{\bullet}$, the semiempirical calculations were carried out at the ROHF level which does not allow for negative spin densities. Since the total spin density must sum to unity, neglect of negative contributions will necessarily underestimate the positive spin densities. We performed, therefore, density functional theory calculations[35] for $HC_{60}^{\bullet}$ and for the five isomers of $HC_{70}^{\bullet}$ at the spin unrestricted level which does allow for negative spin densities using the PM-3 optimized geometries described above. Previous DFT calculations have shown that reliable spin densities can be predicted at this level.[36]

The relative energetics calculated at the non-local DFT (NLDFT) level again show four low-energy isomers (**A** through **D**) and a less stable **E** isomer (Table 4). However, the NLDFT energy difference between the most stable isomer and **E** is only half of that calculated at the PM-3 level. The ordering of the

(32) In ref 8 isomer **A** was found to be the least stable.

(33) Karfunkel, H. R.; Hirsch, A. *Angew. Chem., Int. Ed. Engl.* **1992**, *31*, 1468.

(34) *Cf.* for example: (a) Baker, J.; Fowler, P. W.; Lazzaretti, P.; Malagoli, M.; Zanasi, R. *Chem. Phys. Lett.* **1991**, *184*, 182. (b) Matzusawa, N.; Dixon, D. A. *J. Phys. Chem.* **1992**, *96*, 6241. For an experimental structure, see: Nikolaev, A. V.; Dennis, T. J. S.; Prassides, K.; Soper, A. K. *Chem. Phys. Lett.* **1994**, *223*, 143.

(35) (a) Parr, R. G.; Yang, W. *Density Functional Theory of Atoms and Molecules*; Oxford University Press: New York, 1989. (b) Labanowski, J., Andzelm, J. Eds. *Density Functional Methods in Chemistry*; Springer Verlag: New York, 1991. (c) Seminario, J., Politzer, P., Eds. *Modern Density Functional Theory. A Tool for Chemistry*; Elsevier: Amsterdam, 1995.

(36) See for example: (a) Zheludev, A.; Grand, A.; Ressouche, E.; Schweizer, J.; Morin, B. G.; Epstein, A. J.; Dixon, D. A.; Miller, J. S. *Angew. Chem., Int. Ed. Engl.* **1994**, *33*, 1397; *J. Am. Chem. Soc.* **1994**, *116*, 7243. (b) Lim, M. H.; Worthington, S. E.; Dulles, F. J.; Cramer, C. J. In *Density-Functional Methods in Chemistry*; ACS Symposium Series; Laird, B. B., Ziegler, T., Ross, R., Eds., in press.

Table 5. NLDFT Reaction Energies (kcal/mol) for the Addition of H• to C_2H_4, C_{60}, and C_{70}

	C_2H_4[a]	C_{60}[b]	C_{70}(**A**)[c]	C_{70}(**E**)
ΔE(elec)	−45.9	−49.9	−46.6	−38.8
ΔE(zpe)	5.6			
ΔH(corr)	−1.5			
ΔH_{calc}(298K)	−41.8	−45.8	−42.5	−34.7
ΔH_{exp}(298K)	−36.2 ± 0.8			

[a] $E(C_2H_4) = -78.615552$ au, $E(C_2H_5•) = -79.187109$ au, $E(H•) = -0.498413$ au. [b] $E(C_{60}) = -2286.894078$ au, $E(C_{60}H•) = -2287.472012$. [c] $E(C_{70}\mathbf{A}) = -2668.137992$ au.

most stable isomers at the NLDFT level is different from that at the PM-3 level. The most stable isomer is predicted to be **A** whereas **C**, which was the most stable at the PM-3 level, is now the least stable of the four most stable isomers. Both methods predict that **D** is the second most stable isomer and that **A** is more stable than **B** by about 1 kcal/mol. Geometry optimization at the NLDFT level could change the ordering of the four most stable isomers but would not change the result that **E** is clearly substantially less stable than the other isomers.

The binding energy of a hydrogen to C_{60} and C_{70} can be calculated from the available data (Table 5). First we calculate the energy of binding H• to ethylene to form the C_2H_5• radical as this energy is known experimentally. Furthermore, we can use the calculated zero-point energies for the reaction $C_2H_4 + H• \rightarrow C_2H_5•$ to estimate the corrections for the addition of H• to C_{60} and C_{70}. The calculated value at the BP/DZVP2 level for adding H• to C_2H_4 is −41.8 kcal/mol which is 5.6 kcal/mol more exothermic than the experimental value of −36.2 ± 0.8 kcal/mol.[37] Our calculated values for the addition of H• to C_{60} and C_{70} could similarly be ∼5 kcal/mol too exothermic. For H• + C_{60} our value is 45.8 kcal/mol, which is 4 kcal/mol more energy than released on binding H• to C_2H_4 at this level of calculation. A similar result has been reported for fluorine atom addition to C_2H_4 and C_{60}: the latter was found to be 12 kcal/mol more exothermic than the former.[38] The addition of H• to C_{70} to form the most stable isomer **A** is exothermic by 42.5 kcal/mol and by 34.7 kcal/mol to form the least stable isomer **E**. Thus, H atom addition to C_{70} to form the most stable isomer is less exothermic than the same addition to C_{60}. These results are similar to those reported for the more exothermic addition of fluorine atoms to C_{60} and C_{70}.

The total spin density on each atom, which is obtained by taking the difference between the densities for the α and β electrons, is entered as a percentage number in Figure 5. For the five isomers of HC_{70}• only spin densities greater than 1% are shown, and when these densities belong to carbon atoms on the hidden hemisphere they are shown as smaller numbers near the circled carbon atoms directly above the hidden ones. The shading identifies carbons with greater than 5% positive unpaired spin density. Except for the hydrogen atom, the contributions of the s orbitals to the spin densities are very small. A more pictorial representation for HC_{60}• is presented in Figure 6, which can be compared with the Kekulé structure shown below, where the dark lobes represent positive spin densities and the gray lobes negative densities greater than a practical threshold consistent with clarity. The figure clearly shows that the unpaired spin density resides in radially-oriented p-type orbitals.

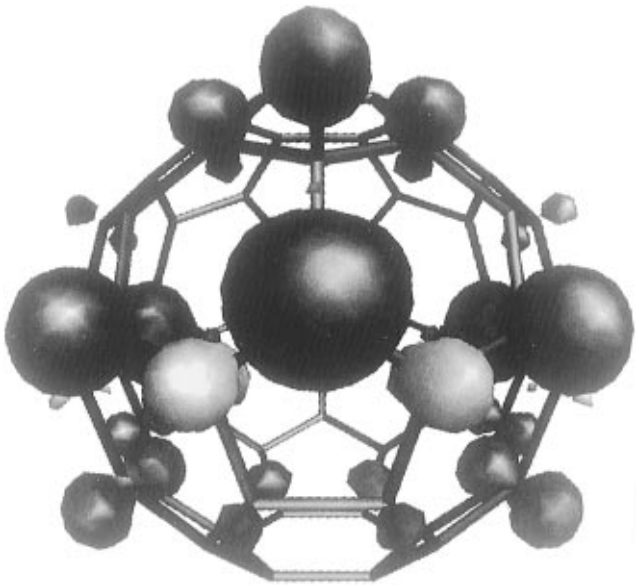

Figure 6. Pictorial representation of the unpaired spin densities in HC_{60}• calculated by density functional theory showing that the unpaired electron resides in radial p-type orbitals on certain carbon atoms. The dark lobes represent positive spin densities and the gray lobes negative spin densities. The orientation of HC_{60}• in this figure matches that of the diagram in the text.

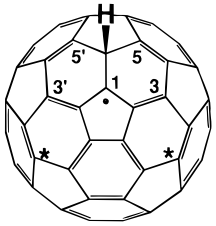

In HC_{60}•, and by extension in RC_{60}• adducts, the highest positive spin density resides on C1 and most of the remaining positive spin density is found on just a few carbon atoms: 3, 3′, 5, 5′, and the carbons marked with asterisks. These are the carbons on which one would place unpaired spin by drawing conventional canonical resonance forms. The highest negative spin densities, on the other hand, reside on carbons 2, 2′, 4, 4′, 6, and the two carbons between carbons 3 and 3′ and the carbons marked with asterisks. This distribution is consistent with ^{13}C ESR data for (*tert*-butyl)C_{60}• which indicated that the unpaired electron cannot be appreciably delocalized beyond the two fused six-membered rings having the alkyl substituent (or the hydrogen atom) at one of the points of fusion.[3a] It is also consistent with the observed 3,6 radical additions across adjacent six-membered rings (more conventionally referred as 1,4 additions) leading to allylic R_3C_{60}• and cyclopentadienyl R_5C_{60}• radicals[39] as the carbons with the second highest spin density are the symmetry-related C3 and C3′, which are diagonally accross the site of initial radical attachment in the six-membered ring. Because of the relative high spin density on the 3,3′ carbons, and the sterical inaccessibility of C1 when the hydrogen is replaced by a bulky alkyl substituent, dimerization of RC_{60}• radicals will occur at these carbon centers.[26]

The unpaired spin distribution in isomer **B** is strikingly similar to that in HC_{60}•. Together with the structural similarity at the polar cap, this indicates that of all isomers **B** is the closest to HC_{60}•. Isomer **A**, which at first glance also resembles HC_{60}•, is really different because the carbon with the highest positive

(37) De More, W. B.; Sander, S. P.; Golden, D. M.; Hampson, R. F.; Kurylo, M. J.; Howard, A. R.; Ravishankara, A. R.; Kolb, C. E.; Molina, M. J. *Chemical Kinetics and Photochemical Data for Use in Stratospheric Modeling. Evaluation No.11*; Jet Propulsion Laboratory, California Institute of Technology: Pasadena, CA, 1994; p 194.

(38) Dixon, D. A.; Smart, B. E.; Krusic, P. J.; Matsuzawa, N. *J. Fluorine Chem.* **1995**, *73*, 209.

(39) Krusic, P. J.; Wasserman, E.; Keizer, P. N.; Morton, J. R.; Preston, K. F. *Science* **1991**, *254*, 1184.

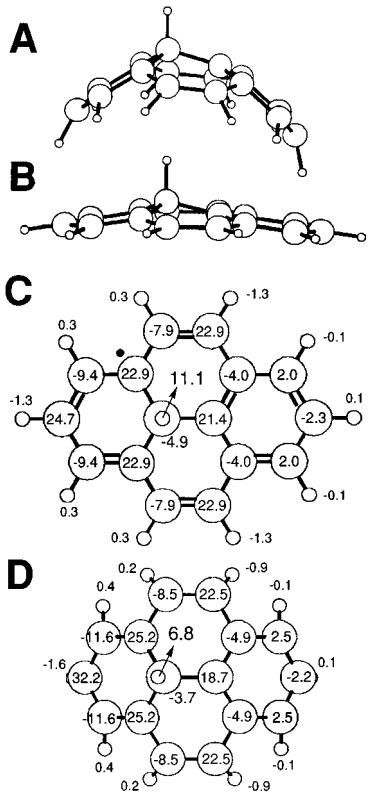

Figure 7. Structural comparison of the spheroidal segment of the **E** isomer of $HC_{70}^{\bullet}$ comprising most of the unpaired spin density (A, with carbon−hydrogen bonds replacing the cut carbon−carbon bonds with d(CH) = 1.09 Å) with the more planar MNDO/PM-3 optimized structure of the radical resulting by H atom addition to the internal carbon of pyrene (B). The projections C of B and D of A show the unpaired spin densities calculated by density functional theory for these radical structures. Projection C also shows the double bonds and the unpaired electron in one of the six canonical resonance structures.

spin density C1 is positioned on the side of the C_{70} ellipsoid with lower overall curvature. The spin density in **A** can thus spread out onto more carbon atoms (without visible effect on the spin density on the hydrogen atom), and a small amount is even predicted to be at the opposite pole.

The cyclohexadienyl nature of **E** is quite apparent from the spin densities in Figure 5E in the equatorial region highlighted with a curved line denoting electron delocalization. On closer inspection, however, the area comprising the majority of the unpaired spin density in **E** resembles much better the yet unknown radical that would result by addition of a hydrogen atom to pyrene. Figure 7 compares the relevant part of isomer **E** (Figures 7A and 7D) dissected from the MNDO/PM-3 optimized structure of $HC_{70}^{\bullet}$(**E**) (with hydrogen atoms (d(CH) = 1.09 Å) replacing the excised carbon atoms) with the MNDO/PM-3 optimized structure of the pyrene H atom adduct (Figure 7B and C) showing one of the six canonical resonance structures. The dramatic difference due to curvature is obvious.

Isomers **C** and **D** have no symmetry and have the most delocalized unpaired electron distribution. **D** is clearly the most delocalized radical of all judging by the many carbon atoms on the opposite hemisphere to that shown in Figure 5 that receive appreciable spin density. Although **D** also has the lowest s-orbital spin density on the hydrogen atom (3.8%) of all isomers, the latter is an imperfect indicator of unpaired electron delocalization since **C**, itself quite delocalized, has a very similar spin density on H to those found for **A** and **B**. Rather, the spin density on the hydrogen atom is an indicator of the spin densities on the adjacent α carbon atoms as discussed below.

Discussion

The existing discussions concerning the assignment of the observed spectra, the electronic structure, and the relative stabilities of the isomeric C_{70} radical monoadducts have centered on the hydrogen atom adducts and on their muonated analogs. The experimental analysis has been hampered, however, by the observation of only four of the expected five regioisomers. With the detection of a fifth muonium−C_{70} adduct[9] and five trifluoromethyl radical adducts of C_{70}, it is appropriate to review some of the arguments presented and to compare the published MO calculations based on semiempirical methods with our density functional theory (DFT) results.

The muonium isotropic hyperfine interactions for all five isomers as well as for $MuC_{60}^{\bullet}$, expressed in Gauss and reduced by the muonium/proton magnetic moment ratio, are compared with the corresponding proton interactions in Table 6. The latter also shows our assignment of the regioisomers labeled with Roman numerals to the structural types labeled with letters **A** through **E**. This assignment is based on the following considerations which will be further justified below.

Isomers **I** and **II** must have either structure **D** or **C** because the latter are the only isomers lacking a plane of symmetry and we have proven that all isomers of type **I** and **II** are without symmetry. All calculations indicate that **D** is the most delocalized $HC_{70}^{\bullet}$ radical, and we assign this structure to **I** since $HC_{70}^{\bullet}$(**I**) and $MuC_{70}^{\bullet}$(**I**) have the smallest proton or muonium hyperfine interactions. Consistent with this assignment, (*tert*-butyl)$C_{70}^{\bullet}$(**I**) and $CH_3C_{70}^{\bullet}$(**I**) also have the smallest ^{13}C coupling for the tertiary carbon of the *tert*-butyl group and for the carbon of the methyl group, respectively.[4,2] This leaves isomers of type **II** with structure **C**. All isomers of type **III** have g factors that are closest to the g factors of their C_{60} analogs and we assign to them structure **B** which is by far the closest to that of $HC_{60}^{\bullet}$. The assignment of **IV** and **V** to **A** and **E**, respectively, is less certain. In making this choice we assumed that the elusiveness of the fifth isomer is probably related to the predicted relative instability of $HC_{70}^{\bullet}$(**E**). We were also influenced by the recent observation of a fifth muonated C_{70} radical which displays the predicted largest hyperfine interaction expected for structure **E** although its size falls short of expectations.

The isotropic muonium−electron hyperfine constant for the fifth muonated C_{70} radical[9] (365.7 MHz) allows one to predict the proton hyperfine splitting of the corresponding, still missing $HC_{70}^{\bullet}$ isomer. Table 6 shows that the muonium couplings, expressed in gauss and reduced by the gyromagnetic μ/H ratio, are on the average 1.103 ± 0.0025 times bigger than the corresponding proton interactions. This increase is due to a substantial vibrational isotope effect[40] caused by the smaller mass of the muon relative to that of the proton (1/9). The vibrational averaging of the hyperfine interaction in the lighter isotopomers will take place over vibrations of wider amplitudes leading to slightly different averages. Reduction of the experimental a(Mu)/3.1834 by the 1.103 factor produces vibrationally corrected values a'(Mu) that can be compared with the a(H) values (Table 6). The excellent agreement for $HC_{60}^{\bullet}$ and four $HC_{70}^{\bullet}$ isomers allows one to predict that the missing fifth $HC_{70}^{\bullet}$ isomer should have a proton hyperfine splitting of 37.2 G at room temperature (Table 6). This agreement also implies that the muonated radicals labeled as in Table 6 are isostructural with all other $RC_{70}^{\bullet}$ regioisomers with the same Roman numeral. It follows that protonated and muonated isomers **I** and **II** cannot

(40) (a) Boxwell, M. A.; Claxton, T. A.; Cox, S. F. J. *J. Chem. Soc., Faraday Trans.* **1993**, *89*, 2957. (b) Morton, J. R.; Negri, F.; Preston. K. F. *Phys. Rev. B* **1994**, *49*, 12446.

Table 6. Comparison of Proton and Muonium Isotropic Hyperfine Splittings (Gauss) and Computational Results for $HC_{60}^{\bullet}$, $MuC_{60}^{\bullet}$, and the Five Isomers of $HC_{70}^{\bullet}$ and $MuC_{70}^{\bullet}$

radical	a(H)	$\frac{a(\mathrm{Mu})^{a,b}}{3.1834}$	a'(Mu)[c]	a(H)[d] (DFT)	R^e (DFT)	R^f (RR)	R^g (AJ)	R^h (MNP)
C_{60}H/Mu	33.1[i]	36.4	33.0	33.1	1.207	0.905	0.83	0.70
					(33.1)[j]	(33.1)[j]	(33.1)[j]	(33.1)[j]
I/D[k]	27.9[i]	30.9	28.0	28.6	0.986	0.508	0.47	0.35
					(27.0)	(18.6)	(18.7)	(16.6)
II/C	34.5[i]	38.1	34.5	35.4	1.120	0.656	0.57	0.46
					(30.7)	(24.0)	(22.7)	(21.8)
III/B	36.0[i]	39.7	36.0	36.1	1.251	0.903	0.84	0.69
					(34.3)	(33.0)	(33.5)	(32.6)
IV/A	36.8[l]	40.5	36.7	36.1	1.258	0.807	0.69	0.61
					(34.5)	(29.5)	(27.5)	(28.8)
V/E	(37.2)[m]	41.0	37.2	54.2	1.775	1.187	1.16	1.10
					(48.7)	(43.4)	(46.3)	(52.0)

[a] Isotropic muonium-electron hyperfine coupling constant expressed in Gauss (2.802 MHz/G) divided by the muon/proton magnetic moment ratio. [b] Reference 9. [c] a(Mu)/3.1834 in column 3 divided by 1.103 to compensate for vibrational effects (see text). [d] DFT spin densities multiplied by 752.27. [e] This work. [f] Reference 30b. [g] Reference 8. [h] Reference 7. [i] Reference 2. [j] Values in parentheses are calculated proton hyperfine splitting from $a^{\mathrm{H}} = kR$ normalized so that the value for $C_{60}H^{\bullet}$ equals the experimental value. [k] Roman numerals denote isostructural $C_{70}H^{\bullet}$ and $C_{70}Mu^{\bullet}$ isomers followed by the structural assignment. [l] From ref 7. [m] Predicted value based on corresponding a'(Mu).

have a plane of symmetry and must be associated with either structure **C** or **D**.

The predicted value of a(H) for isomer **V**/**E** of $HC_{70}^{\bullet}$ (37.2 G) is quite surprising. Since most calculations to date indicate that isomer **E** is the least stable (see Table 4), it has been assumed that the missing isomer would also be of type **E**. For this isomer, however, a substantially larger proton hyperfine interaction was expected on the basis of two types of considerations elaborated below.

The isotropic hyperfine interaction measured in the ESR experiment is proportional to the s character of the MO at a particular nucleus. The DFT spin densities in 1s orbitals of the hydrogens in $HC_{60}^{\bullet}$ and the five isomers of $HC_{70}^{\bullet}$ in Figure 5 can be converted to isotropic hyperfine interactions by multiplication by 504 G, the hyperfine interaction of the isolated hydrogen atom with unit spin density.[41] The values obtained in this manner are systematically too low (*e.g.* 22.2 G for $HC_{60}^{\bullet}$ *vs* 33.1 G experimentally), and they are even lower using the results of semiempirical calculations. Relative to each other, however, they are quite satisfactory for $HC_{60}^{\bullet}$ and the first four isomers of $HC_{70}^{\bullet}$ as can be seen in Table 6 where the DFT H spin densities were scaled so as to obtain agreement with a(H) for $HC_{60}^{\bullet}$ (33.1 G). Only the H hyperfine interaction for isomer **E** is conspicuously too large (54.2 G).

A different approach attempts to estimate the isotropic proton hyperfine interaction from the π spin densities on the adjacent α carbon atoms. Unpaired spin density on β hydrogen atoms, as in the ethyl radical, arises by hyperconjugation and depends on orbital overlap between the singly occupied p-type orbital on the α carbon and the s orbitals on the β hydrogens. Equation 1 has been widely used for simple alkyl radicals: θ is the

$$a^{\mathrm{H}}(\theta) = A + B\cos^2\theta = \rho^{\pi}_{\mathrm{c}}(A' + B'\cos^2\theta) \qquad (1)$$

dihedral angle between the axis of the singly occupied p orbital on the α carbon and the β CH bond direction and ρ^{π}_{c} is the π spin density at the α carbon. The constant A is relatively small and has often been neglected. A value of 50 G has been taken for B for primary radicals while for tertiary radicals a smaller value of 45 G was found more appropriate.[42] As noted by Whiffen[43] and later by Percival and Wlodek,[30a] when there are two α carbon atoms with unpaired spin density, as in the cyclohexadienyl radical, or three as in fullerene radicals, one cannot replace ρ^{π}_{c} simply with the sum of the ρ^{π}_{c}'s of the α carbon atoms. Instead, ρ^{π}_{c} should be replaced with the factor

$$R = (\sum \rho_i^{1/2})^2$$

In other words, one sums the atomic p orbital coefficients and not the spin densities. Since in fullerene radicals θ is necessarily 0°, the proton isotropic hyperfine coupling in the hydrides of C_{60} and C_{70} should be given by eq 2.

$$a^{\mathrm{H}}(\theta) = (\sum \rho_i^{1/2})^2(A' + B') = R(A' + B') \qquad (2)$$

The DFT results in Figure 7 for the almost planar pyrenyl radical and for the curved pyrenyl radical as the model of $HC_{70}^{\bullet}$ (**E**) indicate that the above equation is inadequate. Although the R factors calculated from the DFT spin densities on the three carbons adjacent to the carbon bearing the hydrogen in Figure 7 are similar to each other (2.015 *vs* 2.063), the DFT calculated spin densities on the hydrogens, and therefore the corresponding isotropic couplings, are not (0.111 *vs* 0.068): that for the curved structure is only about half as large as that for the more planar pyrene H adduct. This result has its origin in the much reduced orbital overlap in the curved structure, and it indicates the need for an additional curvature factor k in eq 2 *which will be different for different orbital overlaps and curvatures*.

$$a^{\mathrm{H}}(\theta) = k(\sum \rho_i^{1/2})^2(A' + B') = kR(A' + B') \qquad (3)$$

The R factors calculated with the DFT total spin densities in the radial p-type orbitals on the α carbons in Figure 5 (the s orbital contribution is small) are shown in Table 6 together with the R factors from previous semiempirical calculations. As mentioned above, the latter calculations necessarily seriously underestimate the positive spin densities yielding therefore much lower values of R. To calculate the isotropic H hyperfine interactions from eq 3 (with $A' + B' \sim 45$ G for tertiary radicals), one could estimate a very approximate k from the reduction in proton spin densities for the planar and curved pyrenyl radicals of Figure 7 (k = 6.8/2.063:11.1/2.015 = 0.598). For $HC_{60}^{\bullet}$ we obtain 1.207 × 45 × 0.598 = 32.5 G which, neglecting the temperature dependence of a(H), compares well with the

(41) See for example: Fessenden, R. W.; Schuler, R. H. *J. Chem. Phys.* **1963**, *39*, 2147.
(42) See for example: Krusic, P. J.; Meakin, P.; Jesson, J. P. *J. Phys. Chem.* **1971**, *75*, 3438.
(43) Whiffen, D. *Mol. Phys.* **1963**, *6*, 223.

experimental value of 33.1 G at 340 K.[44] We prefer, however, to calculate $k(A' + B')$ from eq 3 using the experimental a(H) and the calculated R for $HC_{60}^{\bullet}$, and then to multiply the remaining R factors of Table 6 by this value (27.42 G) to obtain the proton hyperfine interactions for the five $HC_{70}^{\bullet}$ isomers. These calculated a(H) values are shown in parentheses under the corresponding R factors in Table 6 for DFT and semiempirical MO calculations. It is seen that the DFT-calculated R factors and the k curvature factor extracted from the data for $HC_{60}^{\bullet}$ account fairly well for the magnitudes and the trend of a(H) of the $HC_{70}^{\bullet}$ isomers except for isomer **E** where a(H) calculated in this fashion is still too large (48.7 G *vs* 37.2 G). The same procedure using the semiempirical R factors by other authors gives less satisfactory results especially in the last column of Table 6.

By using a single curvature or orbital-overlap factor k we tacitly assumed that the curvature in the immediate vicinity of the β carbon bearing the hydrogen is the same for C_{60} and C_{70} hydrides. Consideration of the MNDO/PM-3 optimized structures of $HC_{60}^{\bullet}$ and the $HC_{70}^{\bullet}$ isomers indicates that this assumption is true for $HC_{60}^{\bullet}$ and isomers **A**, **B**, and **C** of $HC_{70}^{\bullet}$, less true for isomer **D**, and inadequate for isomer **E**. As a measure of this curvature we take the average of the three $HC_{\beta}C_{\alpha}$ angles. They are 111.39°, 111.55°, 111.63°, 111.63°, 110.45°, and 108.93° for $HC_{60}^{\bullet}$ and the isomers **A** through **E** of $HC_{70}^{\bullet}$, respectively. It is clear that the curvature at the carbon bearing the hydrogen in **E** is slightly less than for the other hydrides and that we cannot use, therefore, the same curvature factor k for isomer **E** that was used for the other hydrides.[45] There are two other features that set isomer **E** apart from the other hydrides that also affect the orbital overlap determining the β proton isotropic hyperfine interaction and the factor k. One is that the CH fragment in **E** is situated at the fusion of three six-membered rings, whereas in all other hydrides it is situated at the fusion of two six-membered rings and one five-membered ring. This means that the three $C_{\alpha}C_{\beta}C_{\alpha}$ bond angles are more or less equal for **E**, whereas for the other hydrides the bond angle that is part of the five-membered ring is substantially smaller than the other two that are part of six-membered rings. The other feature unique to **E** is that the MNDO/PM-3 geometry optimizations yielded a longer CH bond for **E** (1.123 Å) than for the other hydrides (1.116 ± 0.001). All of this is consistent with our conclusion that a single factor k in the modified Whiffen treatment of a(H) cannot be used for all the $C_{70}H^{\bullet}$ isomers. Parenthetically, the prediction of a longer CH bond for **E** gives credence to our suggestion that radical addition to the equatorial carbons may be reversible under photochemical conditions since it suggests weaker CC bonds connecting the alkyl or fluoroalkyl substituent to the equatorial carbons in $RC_{70}^{\bullet}$.

Our observation of a fifth $CF_3-C_{70}^{\bullet}$ isomer does not provide decisive help in the unambiguous assignment of the observed spectra to specific regioisomers although its high g factor (2.00280) is consistent with expectations for an isomer of type **E** resembling a cyclohexadienyl radical. All $R-C_{70}^{\bullet}$ isomers have g factors that display a substantial positive shift relative to the free electron value of 2.00232 except isomers of type **III** whose g factors are the closest to those of their $R-C_{60}^{\bullet}$ analogs. The latter observation has been used to assign isomers of type **III** to structure **B** which is the most C_{60}-like. A positive g factor shift indicates a mixing of the SOMO with *filled* molecular orbitals connected by the spin−orbit coupling and in this instance can be loosely correlated with delocalization of the unpaired electron. Qualitatively, the latter will lower the energy of the SOMO bringing it closer to the filled MO of appropriate symmetry. This will increase the positive g factor shift since the latter is inversely proportional to ΔE separating the molecular orbitals connected by the spin−orbit interaction. On this basis one would expect the smallest positive g factor shift for isomer **B** which is the least delocalized, although the substantial difference in g factors for **A** and **B** is still puzzling.

In our preliminary report[2] we noted that the positively shifted g factors for isomers of type **IV**, which can be detected easily with aryl and fluoroalkyl radicals but not with simple alkyl radicals, resemble those of related cyclohexadienyl radicals. Indeed, the g factors of cyclohexadienyl (2.00269),[46] 1-phenylcyclohexadienyl (2.00270),[47] and 1-trifluoromethyl-3,5-di-*tert*-butylcyclohexadienyl (2.00290)[48] are remarkably close to those of $HC_{70}^{\bullet}$(**IV**) (2.00274),[7] $C_6H_5C_{70}^{\bullet}$(**IV**) (2.00272), and $CF_3C_{70}^{\bullet}$(**IV**) (2.00283). Furthermore, we noted that phenyl and fluoroalkyl radicals, unlike nucleophilic alkyl radicals, add readily to benzene.[49] On that basis we concluded that isomers **IV** should be identified with the energetically less favored structure **E**, formed under kinetic control, which is essentially a cyclohexadienyl radical resulting by radical addition to the benzene-like equatorial six-membered rings. Having a fifth $CF_3-C_{70}^{\bullet}$ isomer whose g factor (2.00280) is extremely similar to that of isomer **IV** (2.00283) inclines us, not without misgivings, to accept the large g factor difference between isomers **A** and **B** and to assign isomers of type **IV** to structure **A** and the new isomer **V** of $CF_3-C_{60}^{\bullet}$ to structure **E**.

Acknowledgment. We are grateful to S. A. Hill and Miss A. Vincenzi for excellent technical assistance. We dedicate this paper to Fred Tebbe (1934−1995) who, with extraordinary creativity combined with uncommon modesty and kindness, made important contributions to chemistry and DuPont.

JA960979H

(44) Morton, J. R.; Preston, K. F.; Krusic, P. J.; Knight, L. B., Jr. *Chem. Phys. Lett.* **1993**, *204*, 481.

(45) The different curvature or pyramidalization at the different carbons of the parent C_{70} correlates well with the ^{13}C NMR shifts of C_{70}. Thus, the ^{13}C resonance for the least pyramidal E carbon (108.93°) appears as an isolated peak (130.28 ppm) quite upfield relative to the other four A−D signals, all grouped together with similar shifts at much lower field. Within this latter group D is slightly upfield (144.77 ppm) relative to the other three A−C lines (146.82−150.07 ppm) due to the intermediate value for the pyramidalization angle (110.45°). See: Taylor, R.; Hare, J. P.; Abdul-Sada, A. K.; Kroto, H. K. *J. Chem. Soc., Chem. Commun.* **1990**, 1423.

(46) (a) Eiben, K.; Fessenden, R. W. *J. Phys. Chem.* **1971**, *75*, 1186. (b) Eiben, K.; Schuler, R. H. *J. Chem. Phys.* **1975**, *62*, 3093.

(47) Griller, D.; Marriott, P. R.; Nonhebel, D. C.; Perkins, M. J.; Wong, P. C. *J. Am. Chem. Soc.* **1981**, *103*, 7761.

(48) Griller, D.; Dimroth, K.; Fyles, T. M.; Ingold, K. U. *J. Am. Chem. Soc.* **1975**,*97*, 5526.

(49) See for example: (a) Kryger, R. G.; Lorand, J. P.; Stevens, N. R.; Herron, N. R. *J. Am. Chem. Soc.* **1977**, *99*, 7589. (b) Avila, D. V.; Ingold, K. U.; Lusztyk, J.; Dolbier, W. R., Jr.; Pan, H.-Q.; Muir, M. *J. Am. Chem. Soc.* **1994**, *116*, 99. (c) Birchall, J. M.; Irvin, G. P.; Boyson, R. A. *J. Chem. Soc., Perkin Trans. 2* **1975**, 435.